

# Journal of Irrigation and Drainage Engineering

## Analysis of geometrical relationships and friction losses in small diameter lay-flat polyethylene pipes

--Manuscript Draft--

<b>Manuscript Number:</b>	IRENG-7217
<b>Full Title:</b>	Analysis of geometrical relationships and friction losses in small diameter lay-flat polyethylene pipes
<b>Manuscript Region of Origin:</b>	ITALY
<b>Article Type:</b>	Technical Paper
<b>Manuscript Classifications:</b>	94: Hydraulic Measurements; 94.10000: Instrumentation and methods; 97: Irrigation & Drainage; 97.11000: Drip Irrigation
<b>Abstract:</b>	<p>The use of lay-flat polyethylene pipes for microirrigation of horticultural crops has been receiving a widespread attention in the last few decades. The industry has made significant improvements in the hydraulic performance of lay-flat pipes, so that their use is still expected to increase, mainly because of the enhanced competition for water worldwide, that imposes the use of irrigation systems with potentially high application efficiencies and characterized by a limited installation costs.</p> <p>However, even if hydraulic design procedures for conventional microirrigation systems are fairly well established, there is still the need to know how different pipe wall thicknesses of lay-flat pipes can affect the pipe geometry under different operating pressures and the related consequences on friction losses.</p> <p>This paper, after comparing two different procedures, i.e. caliper and photographic method, to assess the geometry of lay-flat polyethylene pipes under different operating pressures, usual in practical applications, analyzes the friction losses per unit pipe length, in order to identify and to assess a procedure for their evaluation.</p> <p>Hydrostatic tests, initially carried out on pipes with wall thicknesses of 0.15, 0.20 and 0.25 mm (6, 8 and 10 mil), evidenced that the pipe vertical and horizontal dimensions measured with both the methods are quite similar, even if the maximum standard deviations associated to the caliper, equal for the three pipes to 0.11 mm, 0.19 mm and 0.10 mm, resulted higher than those obtained with the photographic method, whose values resulted generally lower than 0.06 mm. At the same time, the tests allowed to identify that most of the changes of the pipe dimensions occur in the range of pressure from 0 kPa to about 30 kPa, being the dimensions quite similar at higher values, when the pipes tend to assume a round cross section. When water pressures increase over a certain limit, <math>\Delta p</math>, both vertical width and horizontal height still tend to rise, because of the pipe deformation due to the elasticity of the material, with a trend that resulted more marked for the pipe with the lowest thicknesses. According to the experimental data, the relationships between the pipe effective diameter, to be used to evaluate pipe friction loss, and the water pressure, were then determined on the three considered pipes.</p> <p>On the other side, based on measured friction losses and on pipe effective diameters, it was verified that the relationship between the Darcy-Weisbach friction factor, <math>f</math>, and the Reynolds number, <math>R</math>, can be still described with a power equation in which, by assuming a value of -0.25 for the exponent, the coefficient resulted lower than the theoretical and equal to <math>c=0.285</math>.</p> <p>For the three investigated pipes the errors associated to estimated friction loss per unit pipe length were finally evaluated by considering: i) the experimental relationships between friction factor and Reynolds number and between pipe diameter and operating pressure (case A); ii) the same value of <math>c</math>, but pipe effective diameters of 16.20 mm, 16.10 mm and 15.85 mm corresponding <math>p=\Delta p</math> (case B); iii) the standard procedure, with a value of <math>c=0.302</math> and the pipe diameter equal to 16.10 mm, as suggested by the manufacturer. According to the RMSE values associated to friction factor per unit pipe length, lower for the case A, it was observed that a suitable estimation of friction loss per unit pipe length needs to consider the variations of the pipe effective diameter with water pressure, once disposing of a suitable criterion to estimate the friction factor. On the other hand, incorrect values of pipe diameter combined with an inexact values of the friction factor, generate inaccurate estimations of friction loss, with unavoidable consequences in the pipe design.</p>

1 **Analysis of geometrical relationships and friction losses in small diameter lay-flat**  
2 **polyethylene pipes**

3

4 Giuseppe Provenzano<sup>1</sup>, PhD, Vincenzo Alagna<sup>2</sup>, Dario Autovino<sup>3</sup>, Juan Manzano<sup>4</sup>, PhD, and Giovanni  
5 Rallo<sup>5</sup>, PhD

6

7 <sup>1</sup>Associate Professor, Dipartimento Scienze Agrarie e Forestali, Università di Palermo, Viale delle  
8 Scienze 12, Ed. 4, 90128 Palermo, Italy (corresponding author). E-mail:  
9 [giuseppe.provenzano@unipa.it](mailto:giuseppe.provenzano@unipa.it)

10 <sup>2</sup>PhD Student, Dipartimento Scienze Agrarie e Forestali, Università di Palermo, Viale delle Scienze  
11 12, Ed. 4, 90128 Palermo, Italy. E-mail: [vincenzo.alagna@unipa.it](mailto:vincenzo.alagna@unipa.it)

12 <sup>3</sup>PhD Student, Dipartimento Scienze Agrarie e Forestali, Università di Palermo, Viale delle Scienze  
13 12, Ed. 4, 90128 Palermo, Italy. E-mail: [dario.autovino@unipa.it](mailto:dario.autovino@unipa.it)

14 <sup>4</sup>Professor, Departamento de Ingeniería Rural y Agroalimentaria, Universitat Politècnica de  
15 Valencia, Camino de vera s/n, 46022 Valencia, Spain. E-mail: [juamanju@agf.upv.es](mailto:juamanju@agf.upv.es)

16 <sup>5</sup>Fellowship Researcher, Dipartimento Scienze Agrarie e Forestali, Università di Palermo, Viale delle  
17 Scienze 12, Ed. 4, 90128 Palermo, Italy. E-mail: [giovanni.rallo@unipa.it](mailto:giovanni.rallo@unipa.it)

18

19 **Abstract**

20 The use of lay-flat polyethylene pipes for microirrigation of horticultural crops has been  
21 receiving a widespread attention in the last few decades. The industry has made significant  
22 improvements in the hydraulic performance of lay-flat pipes, so that their use is still expected to  
23 increase, mainly because of the enhanced competition for water worldwide, that imposes the use of  
24 irrigation systems with potentially high application efficiencies and characterized by a limited  
25 installation costs.

26 However, even if hydraulic design procedures for conventional microirrigation systems are fairly

27 well established, there is still the need to know how different pipe wall thicknesses of lay-flat pipes  
28 can affect the pipe geometry under different operating pressures and the related consequences on  
29 friction losses.

30 This paper, after comparing two different procedures, i.e. caliper and photographic method, to  
31 assess the geometry of lay-flat polyethylene pipes under different operating pressures, usual in  
32 practical applications, analyzes the friction losses per unit pipe length, in order to identifies and to  
33 assess a procedure for their evaluation.

34 Hydrostatic tests, initially carried out on pipes with wall thicknesses of 0.15, 0.20 and 0.25 mm (6,  
35 8 and 10 mil), evidenced that the pipe vertical and horizontal dimensions measured with both the  
36 methods are quite similar, even if the maximum standard deviations associated to the caliper, equal  
37 for the three pipes to 0.11 mm, 0.19 mm and 0.10 mm, resulted higher than those obtained with the  
38 photographic method, whose values resulted generally lower than 0.06 mm. At the same time, the  
39 tests allowed to identify that most of the changes of the pipe dimensions occur in the range of  
40 pressure from 0 kPa to about 30 kPa, being the dimensions quite similar at higher values, when the  
41 pipes tend to assume a round cross section. When water pressures increase over a certain limit,  $p_{lim}$ ,  
42 both vertical width and horizontal height still tend to rise, because of the pipe deformation due to  
43 the elasticity of the material, with a trend that resulted more marked for the pipe with the lowest  
44 thicknesses. According to the experimental data, the relationships between the pipe effective  
45 diameter, to be used to evaluate pipe friction loss, and the water pressure, were then determined on  
46 the three considered pipes.

47 On the other side, based on measured friction losses and on pipe effective diameters, it was verified  
48 that the relationship between the Darcy-Weisbach friction factor,  $f$ , and the Reynolds number,  $R$ ,  
49 can be still described with a power equation in which, by assuming a value of -0.25 for the  
50 exponent, the coefficient resulted lower than the theoretical and equal to  $c=0.285$ .

51 For the three investigated pipes the errors associated to estimated friction loss per unit pipe length  
52 were finally evaluated by considering: i) the experimental relationships between friction factor and

53 Reynolds number and between pipe diameter and operating pressure (case A); ii) the same value of  
54  $c$ , but pipe effective diameters of 16.20 mm, 16.10 mm and 15.85 mm corresponding  $p=p_{lim}$  (case  
55 B); iii) the standard procedure, with a value of  $c=0.302$  and the pipe diameter equal to 16.10 mm, as  
56 suggested by the manufacturer. According to the RMSE values associated to friction factor per unit  
57 pipe length, lower for the case A, it was observed that a suitable estimation of friction loss per unit  
58 pipe length needs to consider the variations of the pipe effective diameter with water pressure, once  
59 disposing of a suitable criterion to estimate the friction factor. On the other hand, incorrect values of  
60 pipe diameter combined with a inexact values of the friction factor, generate inaccurate estimations  
61 of friction loss, with unavoidable consequences in the pipe design.

62

63 **Key-words:** Lay-flat polyethylene pipes, Pipe geometry, Hydraulic radius, Friction losses,  
64 Friction factor

65

66

67        **Introduction**

68        Despite lay-flat tubing of different plastic materials have been introduced in the sixties for  
69 irrigation networks, small diameters thin-walled drip-laterals have been recently diffusing, mainly  
70 to irrigate seasonal horticultural crops and with the aim to reduce the installation costs. These drip-  
71 lines, with diameters ranging between 12 mm and 22 mm and co-extruded emitters at different  
72 spacing, are usually manufactured by thin-walled low density polyethylene pipes, so that they are  
73 used under working pressure,  $p$ , generally lower than 150 kPa. Wall thickness varies between 6 mil  
74 and 25 mil, corresponding to 0.15 mm and 0.63 mm, respectively. Compared to the thick-walled  
75 pipes, characterized by wall thicknesses ranging between 0.90 mm and 1.20 mm, which are less  
76 flexible, thin walled pipes become flat when empty, so they can be wrapped in rolls, easier to be  
77 transported (Provenzano et al., 2014).

78        The shape of such pipes and their degree of roundness depend on the pressure of water inside the  
79 pipe: when the working pressure approaches to the lowest limit suggested by the manufacturer, the  
80 pipe cross section tends to become flat, whereas it is round when water pressures exceed a certain  
81 limit.

82        Usually, lay-flat drip irrigation systems are designed by considering conventional methods,  
83 assuming that the pipe cross sections is circular and the internal diameters as provided by the  
84 manufacturers. Only a few years ago, Thompson et al. (2011) emphasized the lack of information  
85 necessary to the accurate design of lay flat drip irrigation systems. These Authors, based on an  
86 experimental analysis carried out by using pipes with wall thickness of 0.125, 0.20, 0.25 and 0.50  
87 mm, evidenced that estimation of friction losses can be improved if the pipe section is still  
88 considered circular, but assuming an effective diameter, lower than the actual, dependent on the  
89 pressure inside the pipe.

90        At increasing operating pressure in fact, the cross-sectional area becomes bigger and, starting  
91 from a quasi-rectangular, it tends to assume a round shape, as showed in fig. 1. These changes  
92 result in a variation of the cross sectional area and can affect the velocity distribution of pipe flow,

93 with the consequence that the velocity distribution along the vertical direction could be different  
94 than the horizontal one. Most of the energy loss is dissipated in the thin layer close to the pipe  
95 (boundary layer), where friction plays an important role; on the other hand, in the region outside  
96 this layer, friction can be neglected (Provenzano et al., 2007). At decreasing water pressure, when  
97 the area and the degree of roundness decrease, the boundary area tends to become larger in  
98 proportion of the cross sectional area (Humpherys and Lauritzen, 1964).

99 Being the friction coefficient dependent on the relative roughness and the velocity distribution,  
100 any change in the shape of the cross section affects both these variables and consequently the  
101 friction losses. At the same time, pressure along the pipe is influenced by both friction losses and  
102 elevation changes. When a lay-flat pipe is laid horizontally, its geometry varies from one section to  
103 another along the flow direction, according to the reduction of pressure head. The flow regime  
104 assumes therefore a steady state condition and friction loss along a certain pipe length is quite  
105 difficult to determine (Rettore Neto et al., 2014).

106 When the flow velocity distribution is known, its average value can be determined by integrating  
107 the velocity profile, so that the flow resistance law can be deduced, as theoretically done by circular  
108 and very wide rectangular shapes, under specific boundary conditions (von Karman, 1934; Prandtl,  
109 1935). According to the Darcy-Weisbach equation, for a circular pipe having an internal diameter  
110 equal to  $d$ , friction loss  $h_f$  along a pipe length  $L$ , can be expressed as:

$$111 \quad h_f = \frac{f V^2}{d 2g} L = \frac{8f Q^2}{g\pi^2 d^5} L \quad (1)$$

112 in which  $f$  is the friction factor,  $V$  the mean flow velocity,  $Q$  the flow rate and  $g$  the acceleration of  
113 gravity.

114 The friction coefficient in smooth pipes is usually evaluated as a function of Reynolds number,  
115  $R$ , by the Blasius equation, valid for quasi-turbulent flow in smooth pipes or similar equations,  
116 specifically obtained for small diameter polyethylene pipe (von Bernuth and Wilson, 1989; Hathoot  
117 et al., 1993; Bagarello et al. 1995; Juana et al., 2002; Provenzano and Pumo, 2004):

118 
$$f = \frac{c}{R^{0.25}} \quad (2)$$

119 in which  $c$  is a constant that, for small diameter polyethylene pipe, can be assumed equal to 0.302  
120 (Bagarello et al. 1997; Provenzano et al., 2005).

121 For low pressure lay-flat drip lines, whose cross section can be non-circular, the internal  
122 diameter  $d$  appearing in eqs. (1) and (2), has to be replaced by a value equal to four times the  
123 hydraulic radius,  $R_h$ , of the new shape (Streeter and Wylie, 1985):

124 
$$d = 4R_h = 4 \frac{A}{P} \quad (3)$$

125 in which  $A$  is pipe cross sectional area and  $P$  is the perimeter of the pipe cross sections. Eq. (3)  
126 provides reasonably precise results for turbulent flow, but it is not very accurate when the flow  
127 regime is laminar (Finnemore and Franzini, 2002). Assuming that for low values of operating  
128 pressure the pipe cross section can be hypothesized as constituted by a circle segment having a  
129 certain radius,  $r$ , mirrored respect to its chord, and subtending an angle  $\omega$  (radians) with the circle  
130 center, the total area,  $A$ , and the wetted perimeter,  $P$ , result:

131 
$$A = r^2(\omega - \text{sen}\omega) \quad (4)$$

132 
$$P = 2\omega r \quad (5)$$

133 Only recently, Rettore Neto et al. (2014) developed a procedure to determine friction loss along  
134 elastic pipe, based on eq. (1) and accounting for the variability of pipe cross section with the  
135 internal water pressure. The new equation, named as “pressure dependent head loss equation”  
136 (PDHLE), needs the knowledge of the modulus of elasticity of pipe material, as well as pipe wall  
137 thickness, working pressure and the variations of internal diameter due to pressure. Anyway, the  
138 proposed methodology takes only into account the elastic deformation of the pipe due to external  
139 forces in a range of internal pressures unusual for practical applications and does not consider the  
140 changes in the shape of pipe cross-section occurring at the lowest operating pressures.

141 A question that still needs to be solved is how different wall thicknesses of lay-flat polyethylene

142 pipes affect the tube geometry under different operating pressures and the related effects on friction  
143 losses.

144 A specific experimental investigation was therefore carried out in order i) to compare two  
145 different procedures, i.e. caliper and photographic method, to measure the pipe horizontal width and  
146 vertical height under different operating pressures; ii) to model the pipe effective diameter as a  
147 function of water pressure and iii) to analyze the values of friction losses per unit pipe length in  
148 deformable polyethylene pipes characterized by different wall thickness, with the aim to identify  
149 and to assess a general procedure for their evaluation.

150

## 151 **Materials and methods**

### 152 *Hydrostatic tests*

153 In order to determine the relationships between the pipe dimensions, i.e. horizontal width and  
154 vertical height, and pressure head, hydrostatic tests were carried out on thin-walled polyethylene  
155 pipes, having nominal diameter,  $ND$ , equal to 16 mm and characterized by three different pipe wall  
156 thicknesses (6 mil, 8 mil, 10 mil). According to the manufacturer, all the pipes have the same  
157 internal diameter,  $d$ , ( $d=16.10$  mm) and should be used under operating pressures ranging between  
158 30 kPa and 100-120 kPa.

159 For each examined pipe, two 1.0 m long sections were connected to two vertical bars, as showed in  
160 fig. 2, and positioned to measure, for different hydrostatic pressures, horizontal width ( $D_h$ ) and  
161 vertical height ( $D_v$ ). Fittings and valves were coupled in such a manner that water could entry in the  
162 tubes and drain from it. At the same time, the corresponding water pressures were measured by  
163 using a mercury gauge equipped with an air vent and connected to the pipes. To reduce the water  
164 pressure in the network, a diaphragm pressure regulating valve was inserted along the inflow pipe.

165 With the aim to eliminate the effect of round end fittings, the horizontal and vertical dimensions  
166 were measured three times in the middle section of the pipes (fig. 2), by means of a digital caliper



167 having a precision of 0.01 mm (caliper method). At the same time two pictures were taken and  
168 used to measure the corresponding pipe dimensions with a CAD software (photographic method).  
169 About thirty measurements for each pipe wall thickness were carried out at least half an hour after  
170 establishing each value of hydrostatic pressure, in order to avoid further pipe deformations. To  
171 increase the accuracy of the measurements, the order of pressure was established randomly and  
172 each determination was repeated twice. Pressure values ranged between about 10 kPa and 150 kPa,  
173 wider than the interval of working pressures suggested by the manufacturer.

174

175

### 176 ***Hydrodynamic tests***

177 Hydrodynamic tests were carried out by using the same three thin-walled polyethylene pipes used  
178 for the hydrostatic ones (*ND* 16), in order to measure friction losses under different pressure heads  
179 and flow rates. The experimental setup, shown in Fig. 3, was fed by a recirculation pump (Ep). A  
180 water tank (T), installed about 20 m below the pipe and a diaphragm pressure regulating valve,  
181 allowed to establish a constant value of pressure head in the hydraulic circuit, in which there were  
182 inserted three trams of pipe, having the same length ( $L=11.8$  m). Two air vents were placed in  
183 correspondence to the differential manometer to facilitate the removal of air bubbles at the begin of  
184 each experiment.

185 Twelve measurements were acquired on each pipe, by considering a wide range of flow rates and  
186 pressure heads, so to obtain an extensive range of Reynolds numbers, usual in practical  
187 applications. The pipe length was also measured to take into account possible longitudinal  
188 dilatations.

189 A differential manometer was used to measure head losses in the three trams in which each pipe  
190 was divided ( $P_1-P_2$ ,  $P_3-P_4$ ,  $P_5-P_6$ ), while a pressure gauge provided the pressure head,  $h_{P1}$ , at the pipe  
191 upstream end (P1). Operating in this way it was possible to dispose, for each pipe thickness, of 36  
192 runs characterized by different geometric and hydraulic conditions. For each operating pressure,

193 head losses, including local losses at fitting connections installed at the upstream and downstream  
194 end of each tram, were measured three times, after reaching a steady state condition. Accuracy of  
195 the pressure gauge readings was equal to 0.05 mmHg, so that the error on measured head loss  
196 resulted about 1.0 mm.

197 During each experiment, the flow discharge, constant through the three trams of pipe, was  
198 measured three time at the downstream end of the circuit, by acquiring the time necessary to fill a  
199 volume of about 10 l; water was weighted with a precision of 0.1 g, and the actual water density  
200 was determined based on the detected temperatures. In order to avoid systematic error, discharges  
201 in experimental tests were assigned randomly (von Bernuth and Wilson, 1989).

202 Table 1 shows minimum and maximum values of pressure head at the upstream end, of flow rate  
203 and of Reynolds number, as measured during the experiments. The latter values were obtained  
204 considering the pipe with a circular cross section, equivalent to the actual measured.

205 With the aim to evaluate the local losses caused by the fitting connectors at the manometric gauges,  
206 a specific experiment was carried out by using the same experimental setup, that was adapted for  
207 the purpose. A short tram of pipe with wall thickness of 8 mil and a length of 0.30 m, was  
208 connected to the manometric gauges ( $P_1$ - $P_2$ ), with the same connectors already used to determine  
209 friction losses. Total pressure losses (friction and local losses) were then measured under pressures  
210 variable from 0.6 kPa to 168.3 kPa and by considering fifteen different flow rates, ranging between  
211 236.1 l/h and 1491.4 l/h. Each determination was repeated three times, in order to reduce  
212 experimental errors. Water temperature was also measured during each experiments, whereas  
213 horizontal and vertical dimensions in the middle cross section of the pipe, were determined once  
214 known the specific relationship between the effective pipe internal diameter,  $d$ , and water pressure,  
215  $p$ . For each flow rate, local losses due to the fittings were then determined by subtracting to the  
216 measured total losses, the corresponding friction losses in the pipe, estimated by assuming the pipe  
217 circular and based on eqs. (1) and (2).

218

219 **Results and discussion**

220 *Hydrostatic tests*

221 For the considered pipes, fig. 4a-c shows the external vertical height,  $D_v$ , and horizontal width,  $D_h$ ,  
222 measured with the photographic method on pipe with wall thicknesses of 6, 8 and 10 mil, as a  
223 function of the corresponding values obtained by the caliper. Horizontal and vertical bars indicate  
224 the standard deviations,  $\sigma$ , of the measurements carried out by means of the two methodologies,  
225 whose values are illustrated in detail in Fig. 5a-c. As can be observed, the values of external pipe  
226 dimensions measured by the photographic method resulted quite similar to the corresponding  
227 obtained with the caliper (fig. 4a-c), even if the latter are generally characterized by higher standard  
228 deviations (fig. 5a-c) than the former. In particular, with the caliper method, the maximum standard  
229 deviation resulted equal to 0.11 mm, 0.19 mm and 0.10 mm for wall thickness of 6 mil, 8 mil and  
230 10 mil respectively, whereas they resulted, at maximum, slightly higher than 0.06 mm when  
231 considering the photographic method.

232 Because of the lower variability characterizing the pipe dimensions measured by the photographic  
233 method compared to the caliper, the following analysis were carried out by considering the former  
234 methodology.

235 Based on the measured values of external pipe dimensions, the corresponding internal width,  $d_h$ ,  
236 and height,  $d_v$ , were then calculated by subtracting twice the pipe wall thickness, equal to 0.15 mm,  
237 0.20 mm and 0.25 mm respectively, for the three considered pipes.

238 Fig. 6a-c illustrates, as a function of water pressure, the variations of internal vertical height and  
239 horizontal width, obtained with the photographic method on pipe with wall thicknesses of 6, 8 and  
240 10 mil. As can be observed, for all the examined cases, the vertical heights rapidly increase,  
241 whereas the horizontal widths decrease, when hydrostatic pressure rises from 0 kPa to about 30  
242 kPa; on the other hands, both the dimensions tend to become similar for the highest values of  
243 hydrostatic pressure and the pipes tend to assume a round cross section ( $d_v=d_h$ ). Moreover, for the  
244 pipes with wall thickness of 6 mil and 8 mil, both  $d_v$  and  $d_h$  tend again to rise when water pressure

245 results higher than a certain threshold values, as a consequence of the pipe deformation due to the  
246 elasticity of the material; as visible, this trend is more marked for the pipe characterized by the  
247 lowest thickness.

248 Fig. 7 shows the degree of pipe roundness obtained, for the examined pipes, by dividing the vertical  
249 height by the horizontal width. As observed by Humphreys and Lauritzen (1962) for  
250 polyvinylchloride plastic and butyl-rubber tubes with diameters ranging between 100 mm and 400  
251 mm, even for low diameter polyethylene pipes, depending on the pressure inside the pipe, the  
252 degree of pipe roundness increases and consequently the pipe cross-sectional area tends rapidly to  
253 inflate, till to reach a round cross section.

254 Based on the measurements of widths and heights in the range of pressures for which pipe is not  
255 circular and assuming the shape of the cross section as constituted by two circle segments, the cross  
256 sectional area and the wetted perimeter were therefore determined by using eqs. (4) and (5). Each  
257 circle segment is characterized by a radius,  $r$ , still variable with the water pressure, that was  
258 evaluated from eq. (5), as a function of the subtended angle  $\omega$  and superimposing that, in the range  
259 of examined pressures, the wetted perimeter  $P$  remains constant.

260 The value of  $\omega$  was obtained by solving, with an iterative procedure, the equation:

$$261 \quad \omega = 2 \arctan \left( \frac{d_h}{2r - d_v} \right) \quad (6)$$

262 whereas the values of the wetted perimeter  $P$  was assumed the one corresponding to the minimum  
263 pressure threshold, to which the pipe become circular.

264 For each water pressure therefore, once identified the shape and determined the cross sectional area  
265 and the wetted perimeter, it was possible to evaluate the hydraulic radius and then, by eq. (3), the  
266 corresponding value of pipe effective diameter to be used in eqs. (1) and (2).

267 Fig. 8 shows the values of the effective diameter,  $d$ , as a function of water pressure,  $p$ . As can be  
268 observed, the values of effective diameters resulted slightly increasing in the ranges of operating  
269 pressure from about 3 to 80 kPa (6 mil), 5 to 100 kPa (8 mil), and 8 to 120 kPa (10 mil), and

270 drastically decrease for water pressures tending to zero. The upper limit of each range,  $p_{lim}$ , for the  
 271 pipe with different thickness, identifies the threshold to which the degree of pipe roundness  
 272 approaches to 1.0. Moreover, due to the elasticity of the material and in agreement with what  
 273 emphasized by Rettore Neto et al. (2014), any further rise of water pressures over  $p_{lim}$ , increase the  
 274 pipe diameters, even if the shape of the cross section remains circular.

275 According to this considerations, experimental  $d(h)$  data pairs were then fitted by curves of  
 276 equation:

$$277 \quad d = a + \frac{b}{p^m} \quad p < p_{lim} \quad (7)$$

278 where a, b and m are the fitting parameters. At the same time, despite the few experimental data  
 279 available, linear functions were used to represent the  $d(p)$  relationships for  $p > p_{lim}$  (Rettore Neto et  
 280 al., 2014):

$$281 \quad d = s + t p \quad p > p_{lim} \quad (8)$$

282  
 283 with s and t fitting parameters. Table 2 shows the values of fitting parameters appearing in eqs. (7)  
 284 and (8), together with the corresponding coefficients of determination. Based on the fitting curves,  
 285 the effective diameters of the 6 mil pipe increased from 16.15 mm to 16.20 mm in the range of  
 286 pressure 3-80 kPa, to reach the value of 16.71 mm for  $p=150$  kPa, whereas, for the 8 mil pipe, the  
 287 effective pipe diameter rose from 16.04 to 16.10 mm for  $5 < p < 100$  kPa, to reach the value  $d= 16.15$   
 288 mm at 150 kPa; on the other side, for the 10 mil pipe, the effective diameter ranged between 15.72  
 289 and 15.85 mm for  $10 < p < 120$  kPa, and remained constant and equal to 15.85 mm, at higher  $p$ . The  
 290 result evidences that, due to the rapid expansion of the cross sections occurring at low pressures,  
 291 even in a range of water pressure lower than the minimum suggested by the manufacturer ( $p < 30$   
 292 kPa), the pipe effective diameters show a more limited variability than the corresponding associated  
 293 to the vertical and horizontal pipe dimensions. This result is consistent with what experimentally  
 294

295 observed by Thomson et al. (2011) on pipes with wall thicknesses ranging between 0.125 mm and  
296 0.500 mm. These Authors evidenced that low thickness polyethylene pipes quite quickly inflate at  
297 very low water pressure reaching an almost constant cross sections, so that proposed to evaluate the  
298 pipe effective diameter according to pre-determined pressure thresholds.  
299 Moreover, the elastic behavior of the pipe recently investigated by Rettore Neto et al. (2014),  
300 occurs only at operating pressure higher than the highest limit suggested by the manufacturer and  
301 only in pipes characterized by a very small wall thickness.

302

### 303 ***Hydrodynamic tests***

304 Following, the results of the friction losses tests for the three considered pipes, are described.  
305 Analysis of friction losses required the preliminary evaluation of head loss in the fittings used to  
306 connect the pipes with the manometric gauges. The results of the related experiments evidenced that  
307 for all the investigated flow rates, local losses caused by the fitting connectors ranged between  
308 92.1% and 94.8% of the measured total losses, being the remaining rate related to the friction losses  
309 in the short tram of pipe used for the tests. Fig. 9 shows, as a function of flow rate  $Q$  [l/h], the  
310 values of local head loss due to the fitting connectors,  $h_l$  [m], that include the local loss due to the  
311 enlargement (upstream connector to pipe) and subsequent contraction (pipe to downstream  
312 connector) of flow streamlines. The following quadratic fitting curve, passing from the origin of  
313 axes, was used to interpolate the experimental  $h_l(Q)$  data pairs:

$$314 \quad h_l = 6 \times 10^{-7} Q^2 + 7 \times 10^{-5} Q \quad R^2=1.00 \quad (9)$$

315 with  $h_l$  in m and  $Q$  in l/h.

316 Once established the way to calculate the local losses due the fitting connectors, for each tram of  
317 the considered pipes, friction losses were evaluated and then referred to the unit pipe lengths. Fig.  
318 10 shows the values of the measured friction loss per unit pipe length,  $J_{meas}$ , as a function of flow  
319 rates, for pipes with wall thickness of 6, 8 and 10 mil. As known, for each considered pipe, the  
320 values of  $J_{meas}$  increase at increasing  $Q$ . Moreover, for a fixed  $Q$ , the corresponding  $J_{meas}$  tends to

321 increase according to the observed reductions of pipe diameter (fig. 8), with differences that  
322 resulted more marked at higher  $Q$ ; at the same time, a certain variability of  $J_{meas}$  is still evident if  
323 considering separately the data collected on the three different pipes. Even this variability has to be  
324 associated to the recognized variations of pipe diameters with the operating pressure.

325 Based on the measured values of  $J_{meas}$  and  $Q$  and disposing of a procedure to determine the pipe  
326 effective diameter as a function of water pressure, the values of the Darcy-Weisbach friction factor  
327 ( $f$ ) associated to each tram of pipe were evaluated by solving eqs. (1), in which the effective  
328 diameters were determined with eq. (7) by considering the average pressure head and neglecting  
329 their variability along the considered tram of pipe. For all the examined pipes, fig. 11 shows the  
330 experimental values of friction factor as a function of Reynolds number. Theoretical values for  
331 laminar ( $f=64/R$  for  $R<2000$ ) and turbulent ( $f=0.302R^{-0.25}$  for  $Re>2000$ ) flow regimes are also  
332 represented. The slightly higher variability of experimental points associated to the lower  $R$ , is  
333 likely due to the incidence or the experimental errors. For the three considered pipes and in the  
334 range of investigated Reynolds numbers, the experimental  $f,R$  data pairs can be fitted by a  
335 relationship, linear in the logarithm graph, that is assumed parallel to the theoretical (eq. 2), but  
336 described by a lower coefficient  $c$ , equal to 0.285.

337 This result seems to conflict with that presented by Thompson et al. (2011) who, working in the  
338 range of Reynolds number between about 1,500 and 10,000 and with lay flat pipes with different  
339 wall thicknesses, obtained values of the friction factor  $f$  systematically higher and characterized by a  
340 greater variability than those obtained in the current investigation, even if differences in  $f$  values  
341 tend to decline at increasing  $R$ . In this regard, as discussed, it is noteworthy that the incidence of  
342 measurements errors increases at decreasing  $R$ . Moreover, these Authors evaluated the values of  $f$   
343 based on pipe effective diameters measured with a caliper that are affected by relatively high  
344 experimental errors. Finally, any difference in the smoothness of pipe used in the two distinct  
345 investigations, could be partially responsible of the discrepancy observed in friction factors.

346 In order to determine the errors on friction loss per unit pipe length associated to the not correct  
347 estimation of the friction factor or to an inexact evaluation of pipe diameter, for all the investigated  
348 pipes, the values of  $J_{est}$  were estimated by three different methodologies and then compared to the  
349 corresponding measured. The first methodology considers a coefficient  $c$  used to evaluate the  
350 friction factors equal to  $c=0.285$  and the empirical relationship between pipe diameter and operating  
351 pressure (eq. 7) (case A); the second takes into account the same value of  $c$ , but assumes as pipe  
352 effective diameters the value of 16.20 mm, 16.10 mm and 15.85 mm determined at  $p=p_{lim}$  (case B),  
353 whereas the third considers the standard procedure, with a value of  $c=0.302$  and the pipe diameter  
354 equal to 16.10 mm, as suggested by the manufacturer.

355 For the three investigated pipes, fig. 12a-c shows the values of friction losses per unit pipe length  
356 estimated in case A, case B and case C,  $J_{est}$ , as a function of the corresponding measured. As can be  
357 observed, the differences between  $J_{meas}$  and  $J_{est}$  in the three considered cases resulted more evident  
358 for the highest values of the variable. The agreement between measured and simulated values was  
359 quantified by means of the Root Mean Square Error, RMSE, that for the three considered pipes,  
360 resulted respectively equal to 0.017, 0.033 and 0.021 for case A, to 0.020, 0.049 and 0.061 for case  
361 B and finally, to 0.050, 0.058 and 0.067 for case C. This statistical parameter has been largely used  
362 (Arbat et al., 2008) and has the advantage of expressing the error in the same units as the variable,  
363 providing more information about the efficiency of the model (Alazba et al., 2012; Legates and  
364 McCabe, 1999).

365 The following fig. 13a-c illustrates, as a function of pressure, the errors on friction loss per unit pipe  
366 length,  $E$ , estimated in the three examined cases. Errors were evaluated as difference between  
367 estimated and measured  $J$ , expressed as percentage of the corresponding measured.

368 As can be observed, in case A, errors resulted generally independent of water pressure and, except  
369 that for sporadic cases mainly associated to the pipe with a wall thickness of 8 mils, they resulted  
370 lower than 5% whereas, for the other two cases, it can be noticed a certain trend with the water  
371 pressure, according to the deformation of the pipes and the consequent variation of their internal



372 diameters. Moreover, the absolute errors associated to both cases B and C, resulted generally higher  
373 that the corresponding associated to case A. This result evidences that to improve estimation of  
374 friction losses per unit pipe length in all the range of operating pressure it is necessary to take into  
375 account the actual variations of pipe diameter and water pressure inside the pipe, as well as to  
376 consider a suitable estimation of the friction factors. On the other hand, assuming the pipe  
377 diameters suggested by the manufacturer and/or unsuitable values of the friction factor, determine  
378 inaccurate estimations of friction loss, with unavoidable consequences in the pipe design.  
379 According to this results, for the accurate design of lay-flat polyethylene pipes, it is therefore  
380 desirable that the manufacturers provide more accurate values of pipe internal diameters, as well as  
381 their variations with the operating water pressure.

382

### 383 ***Conclusions***

384 A comparison between two methodologies to evaluate the dimensions of lay-flat polyethylene pipes  
385 under different operating pressures was initially proposed; then, after analyzing the effects of pipe  
386 geometry on the Darcy-Weisbach friction factor, a procedure to evaluate the pipe friction loss was  
387 suggested.

388 Based on hydrostatic tests carried out on different pipes, characterized by wall thickness of 6 mil, 8  
389 mil and 10 mil, it resulted that both the caliper and the photographic methods are able to detect, the  
390 variability of pipe dimensions with the operating pressure. Anyway, despite the quite similar results  
391 in terms of average pipe dimensions, the measurements carried out with the caliper were  
392 characterized by standard deviations ranging between 0.10 and 0.19 mm, higher than those  
393 associated to the more accurate photographic method that, at maximum, resulted slightly higher  
394 than 0.06 mm. The experimental measurements and the following elaborations evidenced that the  
395 pipe vertical height rapidly increases and the horizontal width decreases with hydrostatic pressures  
396 variable in the range 0-30 kPa, also confirming that the pipe cross sectional area tends to inflate  
397 quite quickly, till reaching its complete roundness. A model was then proposed to represent the

398 effective pipe diameter as a function of water pressure, to be used to evaluate the friction loss. The  
399 model assumed the pipe cross section as constituted by two specular circle segments, with a  
400 constant wetted perimeter, in the range of water pressures lower than 80 kPa, 100 kPa and 120 kPa  
401 to which it was observed the complete roundness of the pipe cross sections. At pressure values  
402 higher than those limits instead, pipe diameter tended to increase linearly with the pressure, with a  
403 trend depending on the elasticity of the material and therefore on pipe thickness.

404 The results of hydrodynamic tests indicated that the friction factor can be more accurately described  
405 by using a power relationship like Blasius equation, but characterized by a coefficient  $c=0.285$  and  
406 therefore lower than those generally used and available in the literature.

407 Finally, analysis of root mean square errors associated to the friction losses per unit pipe length  
408 estimated with three different procedures evidenced that, for the examined pipes, the most accurate  
409 estimation of friction loss per unit pipe length, to which corresponded the lowest RMSE values, can  
410 be obtained by considering the dependence of the effective pipe diameter by the pressure, combined  
411 with the accurate estimation of the friction factor. On the other side, by assuming a constant pipe  
412 diameter leads to a worse estimation of  $J$ , even if associated to the accurate evaluation of the  
413 friction factor. For this reason, it is therefore desirable that manufacturers provide the users with the  
414 pipe geometric data, so that in system design can be taken into account the variability of pipe  
415 diameter with the operating pressure.

416

#### 417 **Acknowledgments**

418 The research was cofinanced by Università di Palermo (FFR 2011) and Ministero dell'Istruzione,  
419 dell'Università e della Ricerca (PRIN 2010). All the Authors setup the research and discussed the  
420 results, while V. Alagna carried out the experimental measurements and G. Provenzano wrote the  
421 paper. A special thank to the Committee for International Relations Office (CORI) of University of  
422 Palermo to support the research cooperation with the University of Valencia.

423

424 **References**

- 425 Alazba, A. A., Mattar, M. A., El Nesr, M. N. and Amin, M. T. 2012. Field assessment of friction  
426 head loss and friction correction factor equations. *J. Irrig. Drain. Eng.*, 138(2), 166-176. DOI:  
427 10.1061/(ASCE)IR.1943-4774.0000387.
- 428 Arbat, G., Puig-Bargues, J., Barragan, J., Bonany, J., and Ramirez deCartagena, F. 2008.  
429 Monitoring soil water status for micro-irrigation management versus modeling approach.  
430 *Biosystems Eng.*, 100(2), 286–296. DOI: 10.1016/j.biosystemseng.2008.02.008.
- 431 Bagarello, V., Ferro, V., Provenzano, G., Pumo, D. 1995. Experimental study on flow resistance  
432 law for small diameter plastic pipes. *J. Irrig. Drain. Eng.*, 121(5), 313-316. ISSN 0733-  
433 8437/85/0005/313-316.
- 434 Bagarello, V., Ferro, V., Provenzano, G., Pumo, D. 1997. Evaluating pressure losses in drip  
435 irrigation lines. *J. Irrig. Drain. Eng.*, 123(1), 1-7. ISSN ASCE. ISSN 0733-9437/197/0001-0001-  
436 0007.
- 437 Finnemore, E.J., and Franzini, J.B. 2002. *Fluid mechanics with engineering applications*. McGraw-  
438 Hill, Boston.
- 439 Hathoot, H.M., Al-Amound, A.T., and Mohammad, F.S. 1993. Analysis and design of trickle  
440 irrigation laterals. *J. Irrig. Drain. Eng.*, 119(5), 756-767. DOI:10.1061/(ASCE)0733-  
441 9437(1993)119:5(756).
- 442 Humphreys, A. S., and Lauritzen, C.W. 1962. Shape factors for hydraulic design of lay-flat drip  
443 irrigation tubing. *Transaction of the ASAE*.
- 444 Humphreys, A. S., and Lauritzen, C.W. 1964. Hydraulic and geometrical relationships of lay-flat  
445 irrigation tubing. Agricultural Research Service. U.S. Department of Agriculture. Washington,  
446 D.C., 20402.
- 447 Juana, L., Rodriguez-Sinobas, L., and Losada, A. 2002. Determining minor head losses in drip  
448 irrigation laterals – I:Methodology. *J. Irrig. Drain. Eng.*, 128(6), 376-384. DOI:  
449 10.1061/(ASCE)0733-9437(2002)128:6(376).

450 Legates, D. R., and McCabe, J. 1999. Evaluating the use of “goodness-of fit” measures in  
451 hydrologic and hydro-climatic model validation. *Water Resour. Res.*, 35(1), 233–241. DOI:  
452 10.1029/1998WR900018.

453 Prandtl, L. 1935. *The mechanics of viscous fluids. Aerodynamic Theory*, (3).

454 Provenzano, G., and Pumo, D. 2004. Experimental analysis of local pressure losses for  
455 microirrigation laterals. *J. Irrig. Drain. Eng.*, 130(4), 318-324. DOI:10.1061/(ASCE)0733-  
456 9437(2004)130:4(318).

457 Provenzano, G., Di Dio, P. M., and Leone, R. 2014. Assessing a Local Losses Evaluation Procedure  
458 for Low-Pressure Lay-Flat Drip Laterals. *J. Irrig. Drain. Eng.*, 140(6), 04014017.  
459 DOI:10.1061/(ASCE)IR.1943-4774.0000731.

460 Provenzano, G., Di Dio, P.M., and Palau Salvador, G. 2007. New computation fluid dynamic  
461 procedure to estimate friction and local losses in coextruded drip laterals. *J. Irrig. Drain. Eng.*,  
462 133(6), 520-527. DOI:10.1061/(ASCE)0733-9437(2007)133:6(520).

463 Provenzano, G., Pumo, D., and Di Dio, P. M. 2005. Simplified Procedure to Evaluate Head Losses  
464 in Drip Irrigation Laterals. *J. Irrig. Drain. Eng.*, 131(6), 525–532. ISSN 0733-9437/2005/6-525–  
465 532.

466 Rettore Neto, O., Botrel, T.A., Frizzone, J.A., and Camargo, A.P. 2014. Method for determining  
467 friction head loss along elastic pipes. *Irrigation Science*. Published online on April, 1, 2014.  
468 DOI:10.1007/s00271-014-0431-7.

469 Streeter V.L., and Wylie, E.B. 1985. *Fluid mechanics*. 8th ed. McGraw-Hill, New York.

470 Thompson, E., Merkley, G., Keller, A., and Barfuss, S. 2011. Experimental determination of the  
471 hydraulic properties of low-pressure, lay-flat drip irrigation systems. *J. Irrig. Drain. Eng.*,  
472 137(1), 37-48. DOI:10.1061/(ASCE)IR.1943-4774.0000269, 37–48.

473 von Karman, T. 1934. Turbulence and skin friction. 1. *Aeronautical Sci.*, 1(1).

474 Von Bernuth R.D., and Wilson, T. 1989. Friction factor for small diameter plastic pipe. *J. Hydr.*  
475 *Eng. ASCE*, 115(2).

Table 1 – Minimum and maximum pressure at the pipe upstream end,  $h_{p1}$ , and flow rate,  $Q$ , measured during the experiments carried out on pipes with wall thickness of 6 mil, 8 mil and 10 mil. The range of Reynolds number,  $R$ , and the lengths of the three trams of pipe are also indicated.

Wall thickness	$h_{p1}$ [kPa]		$Q$ [l/h]		$R$ [-]		$L$ [m]
	min	max	min	max	min	max	
6 mil	8.4	173.0	142.0	944.5	3146.0	20435.0	11.84
8 mil	2.4	175.5	144.4	1114.6	3167.0	24231.0	11.83
10 mil	11.9	174.1	158.7	922.3	3513.0	20400.0	11.83

Table 2 – Parameters of eqs. (7) and (8) and coefficients of determination, obtained for the considered pipes. The ranges of pressure variability define the limits of models application.

Wall thickness	Range p [kPa]	a	b	m	R <sup>2</sup>	Range p [kPa]	s	t	R <sup>2</sup>
		$d = a + b p^{-m}$					$d = s + t p$		
6 mil	0-80	16.213	-0.121	0.525	0.82	80-150	15.507	0.008	0.99
8 mil	0-100	16.109	-0.241	0.753	0.97	100-150	15.951	0.001	0.88
10 mil	0-120	15.864	-0.980	0.833	0.92	120-150	15.850	0.000	-

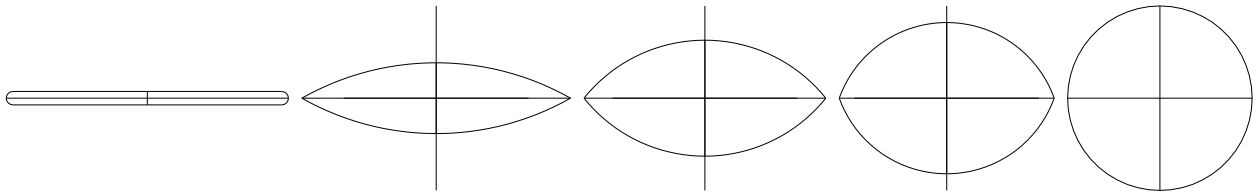


Fig. 1 – Possible qualitative shapes of lay-flat pipe cross sections at increasing water pressure (from quasi-rectangular to circular).

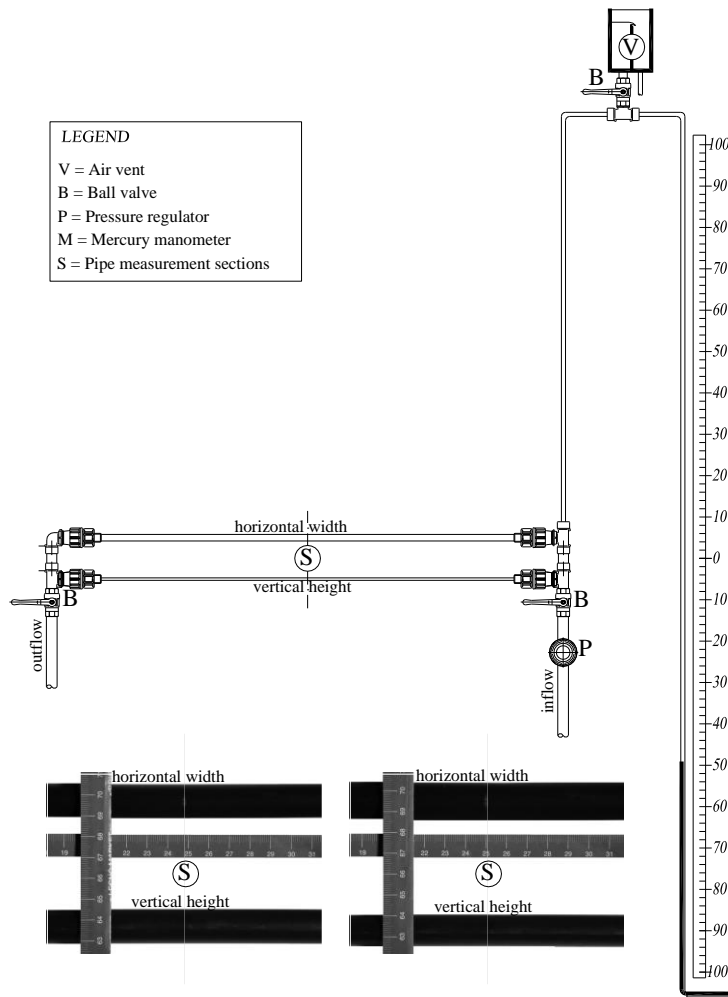


Fig. 2 – Layout used for hydrostatic tests, to determine the relationships between pipe dimensions and pressure head. Two examples of pictures, taken at different pressure heads, are also shown.



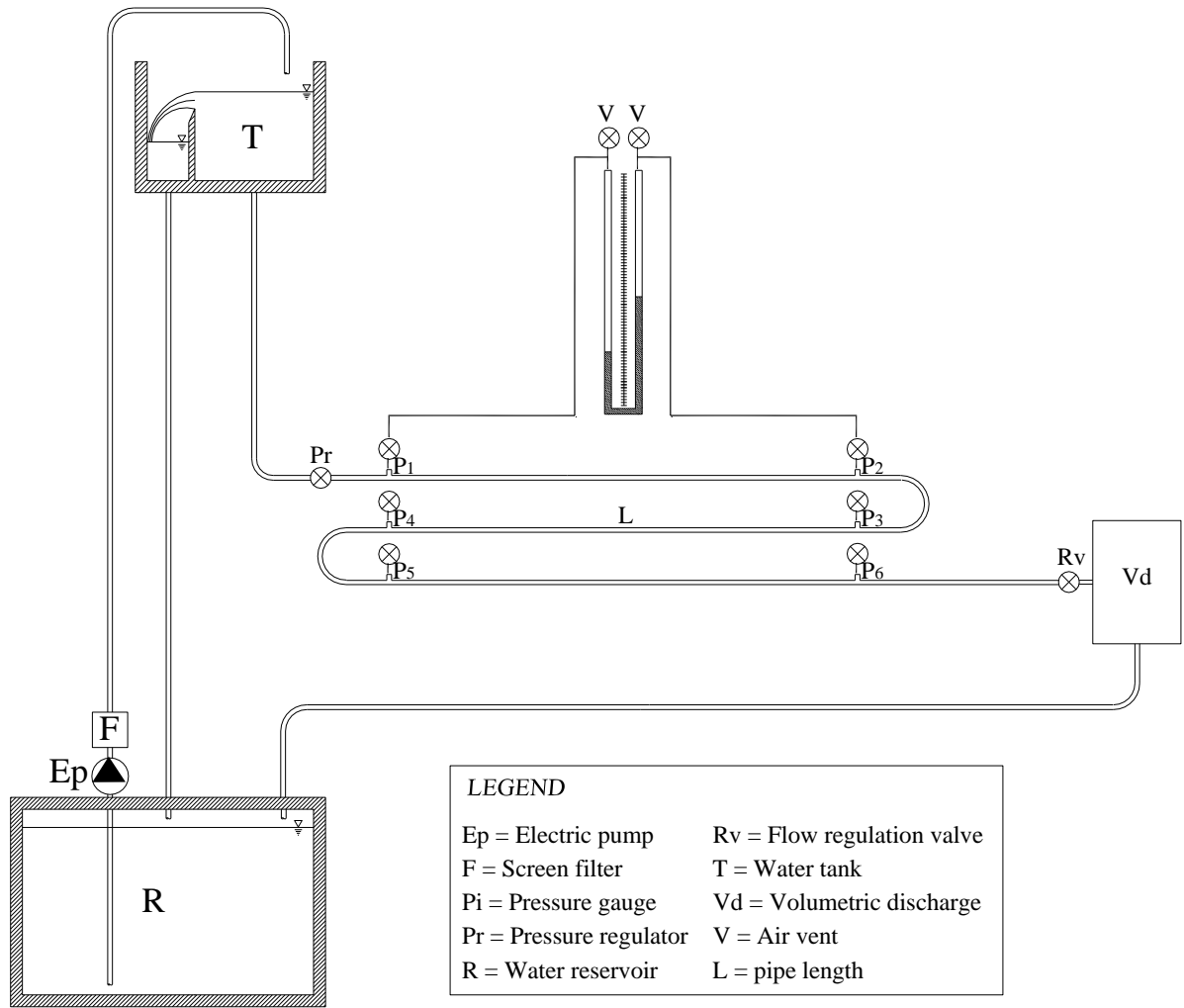
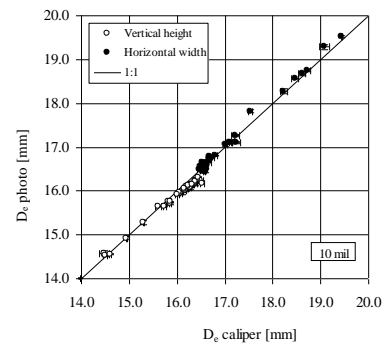
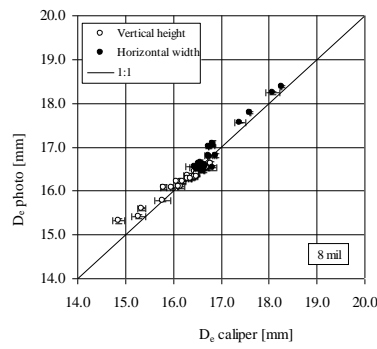
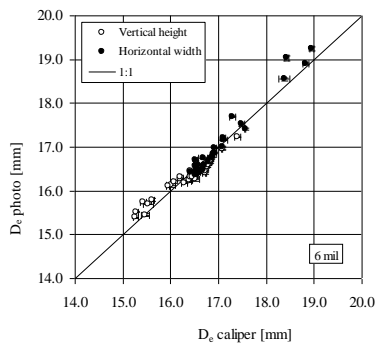


Fig. 3 – Layout used for the hydrodynamic tests.

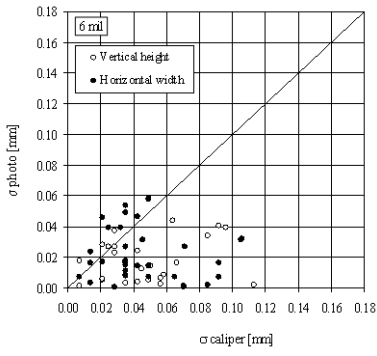


a)

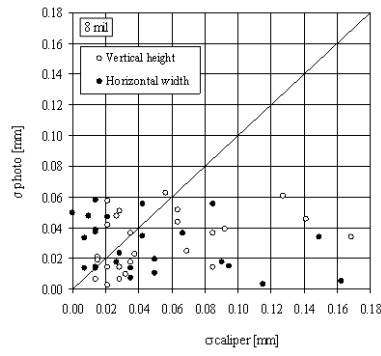
b)

c)

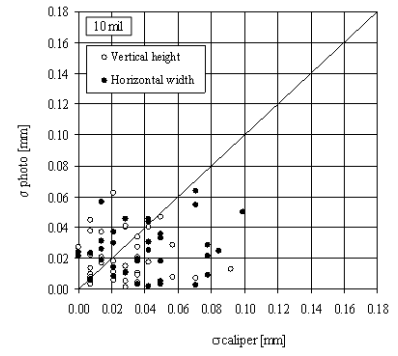
Fig. 4 a,b,c – Vertical and horizontal external pipe dimensions measured with the photographic method as a function of those measured by the caliper. The tested pipes, having ND of 16 mm, are characterized by wall thickness of 6, 8 and 10 mil. Horizontal and vertical bars indicate the standard deviations of the measured values.



a)



b)



c)

Fig. 5a,b,c – Standard deviation,  $\sigma$ , of vertical and horizontal external pipe dimensions measured with the photographic method as a function of the corresponding measured by the caliper for pipe wall thickness of 6, 8 and 10 mil.



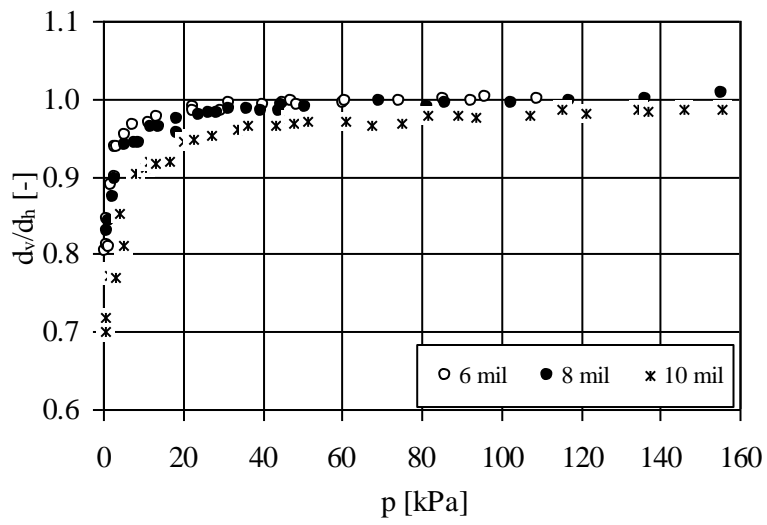


Fig. 7 – Degree of pipe roundness evaluated on pipe with wall thickness of 6, 8 and 10 mil.

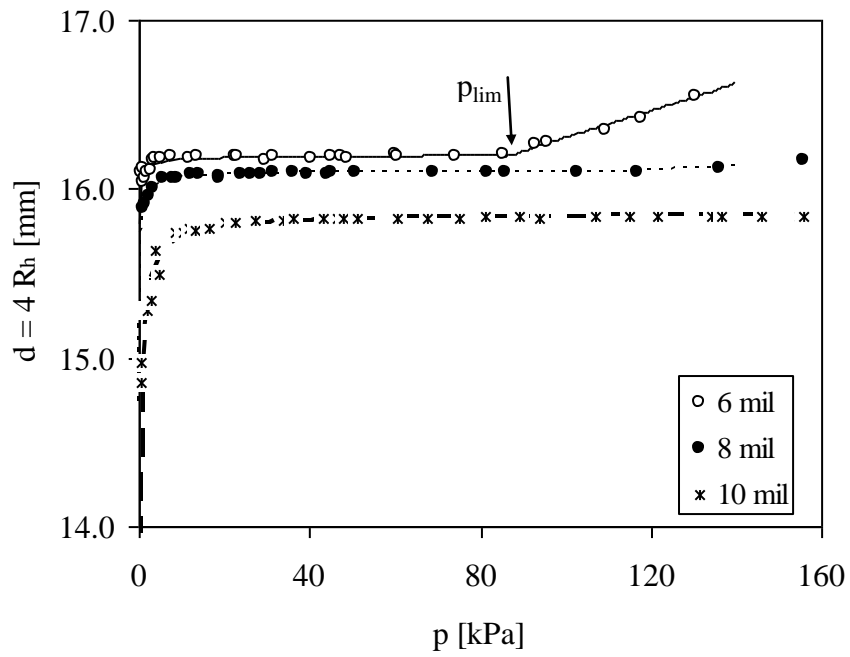


Fig. 8 – Values of the average internal pipe diameter,  $d$ , evaluated by eq. (3), as a function of water pressure, for pipe wall thickness of 6, 8 and 10 mil and related fitting curves.

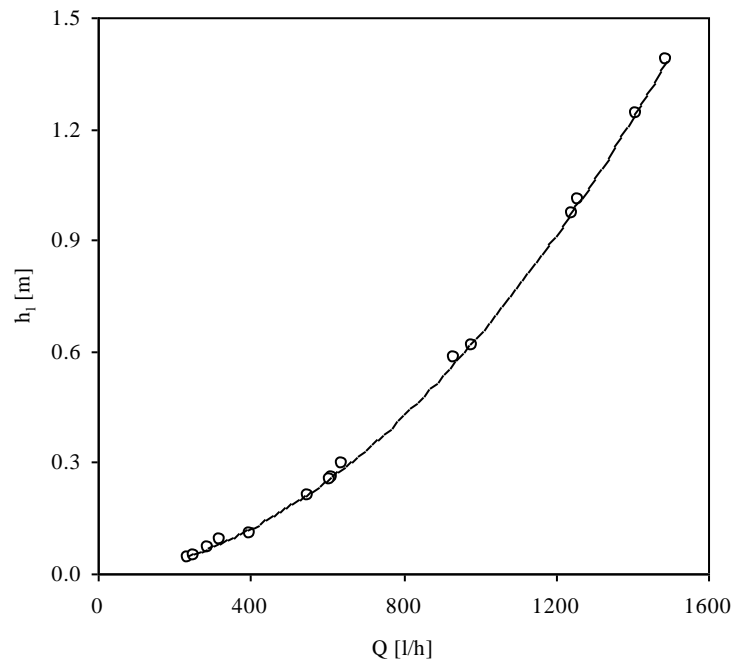


Fig. 9 – Experimental values of local losses due to the fitting connectors as a function of flow rates. The associated fitting curve, represented by eq. (8), is also shown.

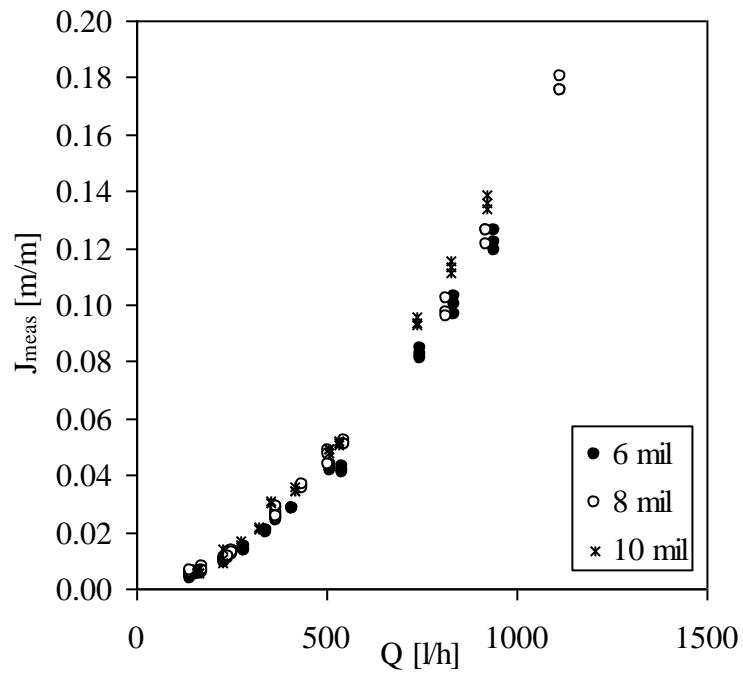


Fig. 10 – Measured friction losses per unit pipe length as a function of flow rates, for pipes with wall thickness of 6, 8 and 10 mil.



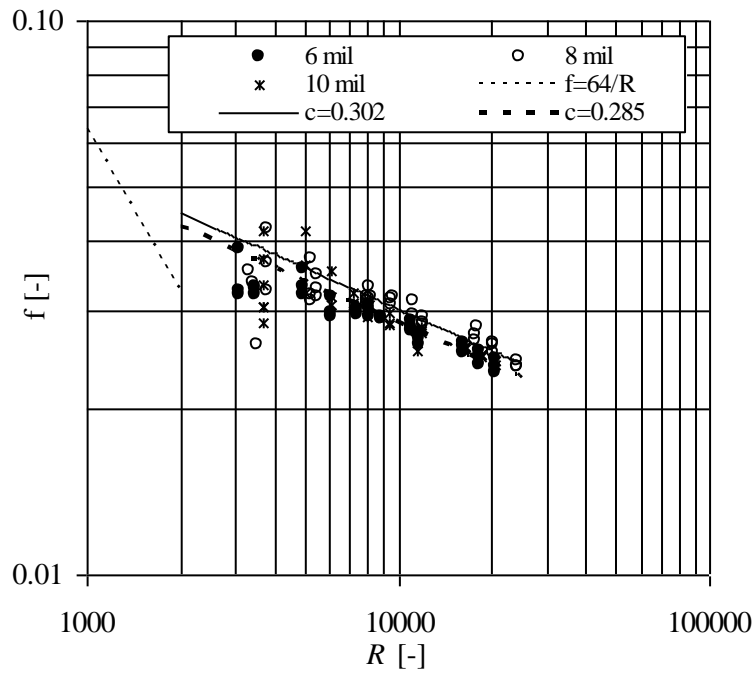
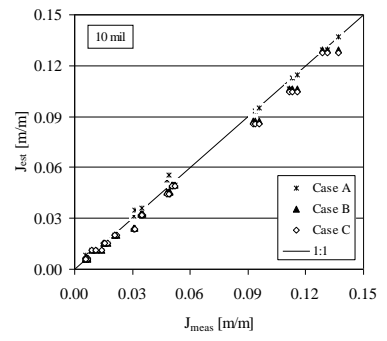
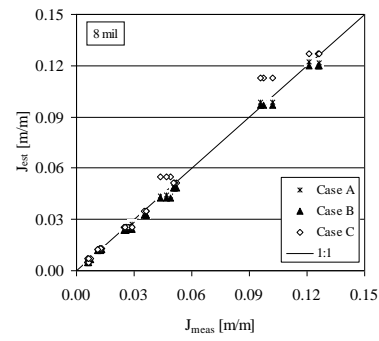
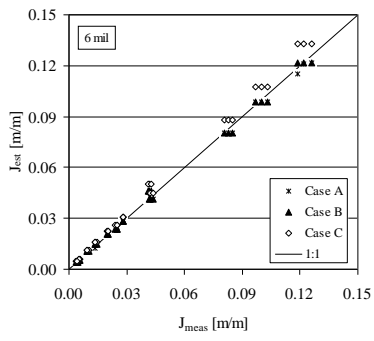


Fig. 11 –Darcy-Weisbach friction factor as a function of Reynolds number for the examined pipes and related fitting equation (eq. 9). Theoretical values for laminar ( $R < 2000$ ) and for turbulent ( $Re > 2000$ ) regimes are also shown.

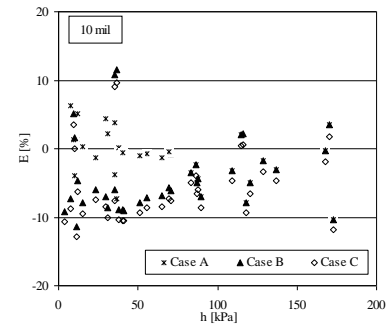
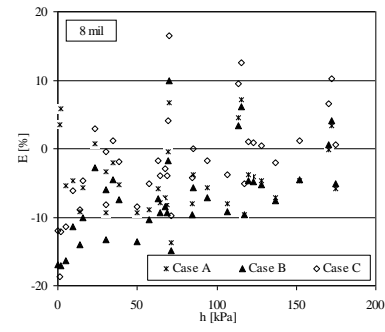
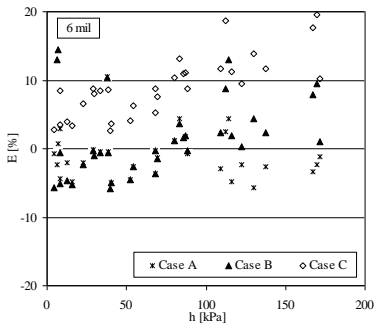


a)

b)

c)

Fig. 12a,b,c – Friction losses per unit pipe length estimated in case A, case B and case C, as a function of the corresponding measured on the investigated pipes.



a)

b)

c)

Fig. 13a,b,c – Errors associated to the estimated friction losses in case A, B and C obtained for the three considered pipes.

## FIGURE CAPTIONS

Fig. 1 – Possible qualitative shapes of lay-flat pipe cross sections at increasing water pressure (from quasi-rectangular to circular).

Fig. 2 – Layout used for hydrostatic tests, to determine the relationships between pipe dimensions and pressure head. Two examples of pictures, taken at different pressure heads, are also shown.

Fig. 3 – Layout used for the hydrodynamic tests.

Fig. 4 a,b,c – Vertical and horizontal external pipe dimensions measured with the photographic method as a function of those measured by the caliper. The tested pipes, having ND of 16 mm, are characterized by wall thickness of 6, 8 and 10 mil. Horizontal and vertical bars indicate the standard deviations of the measured values.

Fig. 5a,b,c – Standard deviation,  $\sigma$ , of vertical and horizontal external pipe dimensions measured with the photographic method as a function of the corresponding measured by the caliper for pipe wall thickness of 6, 8 and 10 mil.

Fig. 6a,b,c – Variations of internal pipe dimensions obtained with the photographic method as a function of water pressure, for pipe wall thickness of 6, 8 and 10 mil.

Fig. 7 – Degree of pipe roundness evaluated on pipe with wall thickness of 6, 8 and 10 mil.

Fig. 8 – Values of the average internal pipe diameter,  $d$ , evaluated by eq. (3), as a function of water pressure, for pipe wall thickness of 6, 8 and 10 mil and related fitting curves.

Fig. 9 – Experimental values of local losses due to the fitting connectors as a function of flow rates. The associated fitting curve, represented by eq. (8), is also shown.

Fig. 10 – Measured friction losses per unit pipe length as a function of flow rates, for pipes with wall thickness of 6, 8 and 10 mil.

Fig. 11 – Darcy-Weisbach friction factor as a function of Reynolds number for the examined pipes and related fitting equation (eq. 9). Theoretical values for laminar ( $R < 2000$ ) and for turbulent ( $R > 2000$ ) regimes are also shown.

Fig. 12a,b,c – Friction losses per unit pipe length estimated in case A, case B and case C, as a function of the corresponding measured on the investigated pipes.

Fig. 13a,b,c – Errors associated to the estimated friction losses in case A, B and C obtained for the three considered pipes.